

# Multi-wavelength activity of blazar 3C 454.3 in 2013 September

D.A. Morozova<sup>1</sup>, V.M. Larionov<sup>1</sup>, S.G. Jorstad<sup>1,2</sup>, A.P. Marscher<sup>2</sup>, I.S. Troitskiy<sup>1</sup>, D.A. Blinov<sup>3,1</sup>, N.V. Efimova<sup>4</sup>, V.A. Hagen-Thorn<sup>1</sup>, A. A. Arkharov<sup>4</sup>, P.S. Smith<sup>5</sup>  
<sup>1</sup>Astronomical Institute of SPbSU, <sup>2</sup>IAR BU, <sup>3</sup>University of Crete, Greece, <sup>4</sup>Pulkovo Observatory, <sup>5</sup>Steward Observatory

## Abstract

We present the results of a series of optical and infrared observations of the FSRQ 3C 454.3 carried out during 2013 September-October optical flare. Multicolor optical observations were obtained at 0.4 m telescope of SPbSU (LX200), the 0.7 m telescope of the Crimean Astrophysical Observatory (AZT-8), the 1.8 telescope of the Lowell observatory (Perkins) and infrared observations were obtained at 1 m telescope of Campo Imperatore (AZT-24). We found nonlinear dependence of flux-flux relations for optical and NIR bands during this flare. The optical and infrared flares were contemporaneous with simultaneous flare in gamma-rays. The optical EVPA shows a smooth intranight rotation with the amplitude of 20 degrees over 4 nights (24 - 27 September). Such intranight EVPA variations could be the signature of hierarchical helical structure: finer structure, responsible for rapid intranight variation, and the large-scale one, responsible for long-term (months) variability.

## 1. Introduction

The blazar 3C 454.3 ( $z=0.859$ ) is a quasar, which is well known for pronounced variability at all wavelengths, from the radio to the  $\gamma$ -ray band. Its optical variability was analyzed by Hagen-Thorn et al. (2009, 2013) and Raiteri et al. (2008), who found SED changes between flares. Comprehensive analysis of radio to gamma-ray behavior was performed in Jorstad et al. (2013), who discovered a tight connection between events at these wavelengths.

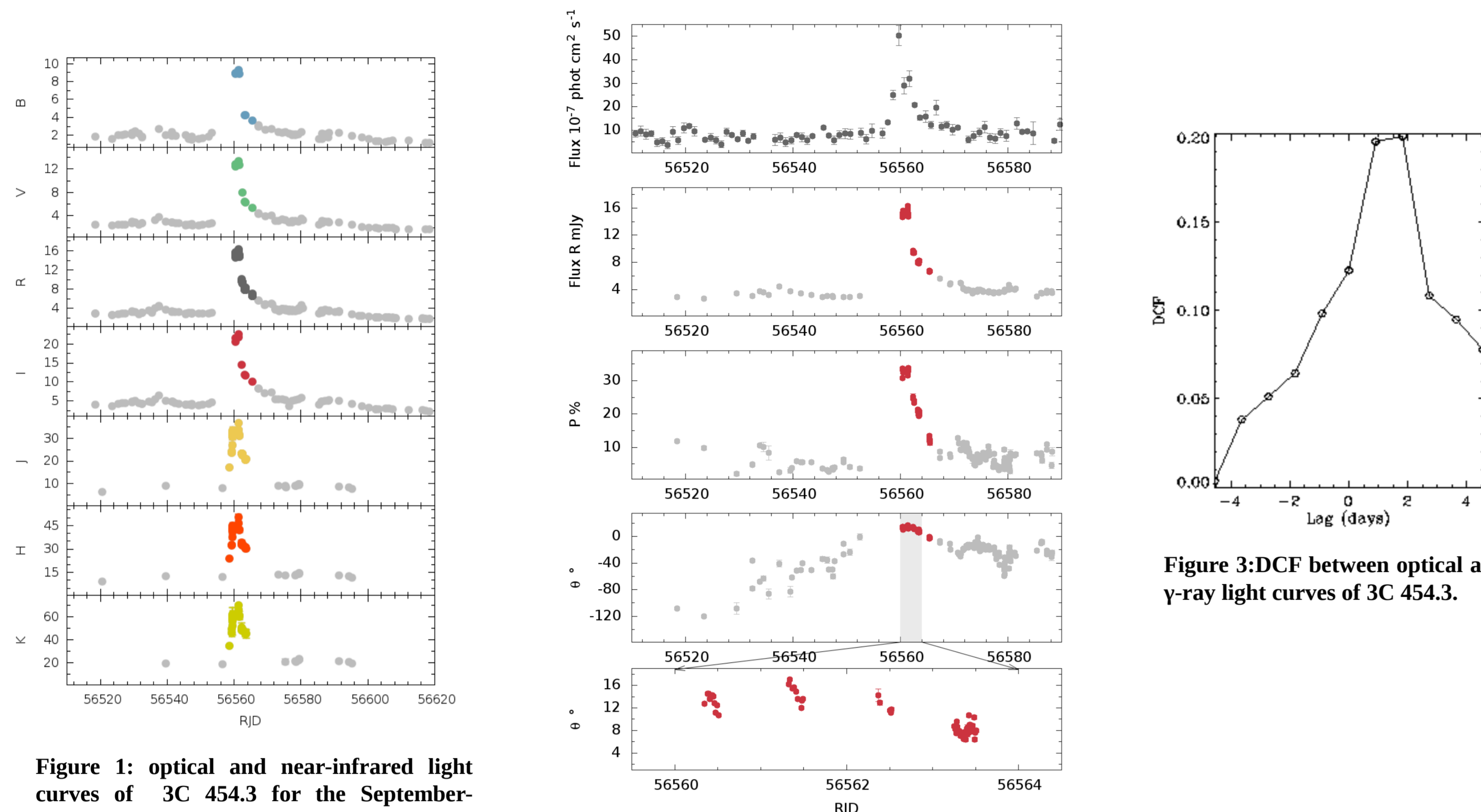


Figure 1: optical and near-infrared light curves of 3C 454.3 for the September-October 2013.

Figure 2: from top to bottom:  $\gamma$ -ray flux, optical flux density (corrected for Galactic extinction), fractional polarization, and position angle of polarization in R band vs. time in 2013 September-October; bottom panel is a blowup of four days 24, 25, 26, 27 September

Figure 3: DCF between optical and  $\gamma$ -ray light curves of 3C 454.3.

## 2. Observations and data reduction

In this paper we use simultaneous photometric and polarimetric measurements of 3C 454.3 obtained over 100 days.

### Optical and near-infrared photometry

We carry out optical BVRI observations at the 70-cm AZT-8 reflector (Crimean Astrophysical Observatory, Russia), 40-cm LX-200 telescope (St. Petersburg, Russia) and 180-cm Perkins telescope (Lowell observatory, USA). The near-IR JHK data were obtained at AZT-24 (Campo Imperatore, Italy).

The optical and near-infrared light curves of 3C 454.3 are shown in Fig.1. The Optical and infrared flares are simultaneous. The observations reported here were collected as a part of a long-term multi-wavelength study of a sample of  $\gamma$ -ray bright blazars. For the whole sample of observations visit our website.

### Optical polarimetry

Polarimetric observations were collected in St. Petersburg University (Crimea and St. Petersburg), Lowell (Perkins), Steward and University of Crete (Robopol) observatories. To correct for the interstellar polarization, the mean relative Stokes parameters of nearby stars were subtracted from the relative Stokes parameters of the object. This accounts for the instrumental polarization as well, under the assumption that the radiation of the stars is unpolarized. The errors in the degree of polarization,  $P$ , are less than 1% (in most cases less than 0.5%), while the electric vector position angle (EVPA),  $\theta$ , is determined with an uncertainty of  $1-2^\circ$ . We solved the  $\pm 180^\circ$  ambiguity adding/subtracting  $180^\circ$  each time that the subsequent value of EVPA is  $>90^\circ$  less/more than the preceding one.

Fig. 2 presents the flux and polarization behavior of 3C 454.3 for 2013 September-October. The degree of polarization exceeded  $\sim 30\%$  at the maximum, and was mostly  $\leq 1.5\%$  during quiescence.

### Gamma-ray Observations

We derive  $\gamma$ -ray flux densities at 0.1-200 GeV by analyzing data from the Fermi Large Area Telescope (LAT), provided by the Fermi Science Space Center using the standard software Abdo et al. (2010). The  $\gamma$ -ray light curves were constructed with a binning size of 1 day, and a detection criterion that the maximum-likelihood test statistic (TS) should exceed 10.0. Gamma-ray light curve is shown on top panel of Fig.2.

We calculate the discrete correlation function (DCF, Edelson & Krolik 1988) of the optical and  $\gamma$ -ray flux variations of 3C 454.3 for September-October 2013. The results are given in Fig.3. Gamma-ray light curve leads optical by  $\sim 2$  days, but this lag is within the DCF half-width.

## 3. Results and Discussion

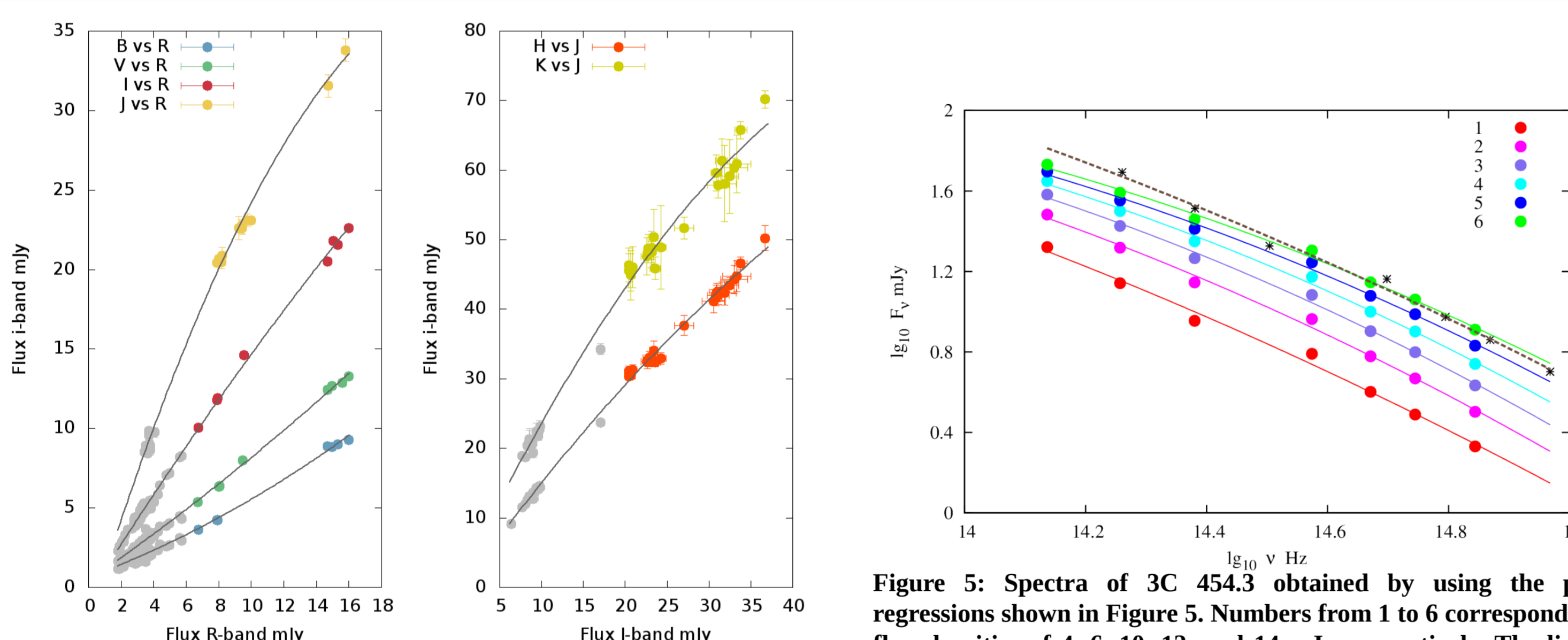


Figure 4: De-reddened flux-flux dependencies in the optical-NIR region. The red lines represent second-order polynomial regressions.

Figure 5: Spectra of 3C 454.3 obtained by using the polynomial regressions shown in Figure 5. Numbers from 1 to 6 correspond to R-band flux densities of 4, 6, 10, 12, and 14 mJy, respectively. The lines tracing each spectrum represent a polynomial regression. Brown dashed curve is the result of the shift of spectrum 1 toward spectrum 6 when  $\delta$  changes by a factor of 1.33.

### Color evolution

We used method suggested in a number of papers of Hagen-Thorn and co-workers (see Larionov et al. (2008, 2010) to study color evolution of the source. The method is based on plotting of (quasi)simultaneous flux densities in different color bands. An example of such approach is given in Fig.4, where the flux densities in B, V, I and J bands are plotted against R, and H and K - against J band flux densities. The flux-flux relations show complex non-linear relations that can be fitted by second-order polynomials  $a + b \cdot F_R + c \cdot F_R^2$  or  $a + b \cdot F_J + c \cdot F_J^2$ . The concavity of the regression is always directed toward the higher frequency band, thus clearly displaying a bluer-when-brighter type of variable source behavior. Hagen-Thorn et al. (2009, 2013) and Raiteri et al. (2008) found that during the number of flares object demonstrates both redder- and bluer-when-brighter trend. The difference in SED during flares might originate due to a new variable component (e.g. shock), which becomes dominant at the highest flux stage. The component possesses its own electron energy distribution.

In order to get SED of the variable source we use estimates of the constant source contribution derived by Hagen-Thorn et al. (2013). Simultaneous spectra of the variable source in 3C 454.3 for 6 selected flux densities in R from 4 to 14 mJy are shown in Fig.5. Since  $F_\nu \sim \delta^{p+c}$ , we can use  $F_{\max}/F_{\min}$  relation to estimate  $\delta_{\max}/\delta_{\min}$ . If we accept  $p=3$  (for a moving source),  $\alpha_{\text{mean}} \sim 1.1$  (see Fig.5), and R-band flux changes from 5.7 to 15 mJy, we get  $\delta_{\max}/\delta_{\min} \sim 1.26$ .

Since  $F_\nu(v) = \delta^p \cdot F_\nu'(v')$  and  $v = \delta \cdot v'$ , in logarithmic scale (as in Fig. 5) changes of  $\Delta \log \delta$  in the Doppler factor lead to a shift of the spectrum by  $\Delta \log v = \Delta \log \delta$  (in the frequency direction) and  $\Delta \log F_\nu = p \cdot \Delta \log \delta$  (in the flux direction).

The brown dashed spectrum in Fig.6 has been obtained from spectrum 1 by increasing  $\delta$  by a factor of 1.33 in proposition that the flux increase is caused only by  $\delta$  increase. It reproduces the high frequency part of the "real" spectrum 6 quite good, but there is a lack of infrared photons in the low frequency part.

## 4. Conclusions

The analysis of photopolarimetric data collected in 2013 September-October, led us to following conclusions:

- Simultaneity of optical, infrared and  $\gamma$ -ray flares suggests that the activity in these bands arises in co-spatial region.
- During the flare in 2013 October 3C 454.3 showed a bluer-when-brighter trend. Both bluer- and redder-when-brighter trends were observed for 3C 454.3 previously. Such behavior could be explained by appearance of a new variable component with the specific, different for every outburst event, electron energy distribution.
- An increase of the polarization degree along with the flux level might be a signature of shock processes leading to increased ordering of the magnetic field in the shocked region as compared to less ordered field in the quiescent jet.
- Intranight EVPA variations could be the signature of hierarchical helical structure: finer structure is responsible for EVPA variations during night and the large-scale one for months-lasting activity.

## Acknowledgments

This work was partly supported by grants of RFBR (6.15.282.2015) and St.Petersburg University (6.38.335.2015, 6.41.657.2015, 6.41.673.2015).

### Polarimetric behavior

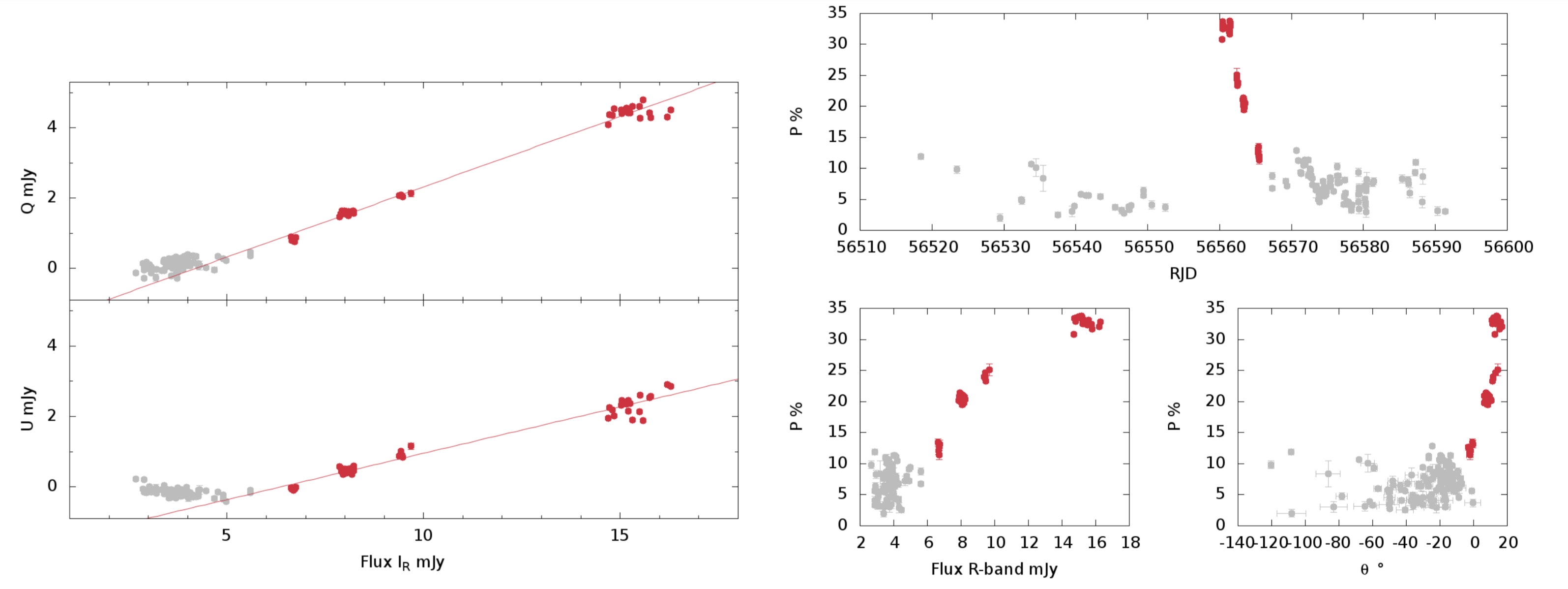


Figure 6: absolute Stokes parameters variation during 2013 September-October; top: Stokes Q vs. I, bottom: Stokes U vs. I. Red color refer to 4 nights 24, 25, 26 and 27 September.

Figure 7: the relation between degree of polarization vs. Time (top panel), degree of polarization vs. R-band flux (bottom left), degree of polarization vs. EVPA (bottom right).

Fig.2 displays the entire set of optical photometric and polarimetric data. From the visual inspection of the figure it is immediately seen that the polarization degree exceeded 30%, which is rather high. During quiescence the optical EVPA rotates from  $-120^\circ$  to  $\sim 0^\circ$  that might be precursor of the flare. At the maximum of the flare EVPA is around  $20^\circ$ , which is close to EVPA of the radiocore at 43 GHz at the nearest date ( $\sim 30^\circ$ , 18 November 2013).

Following Hagen-Thorn & Marchenko (1999), we plotted (Q vs I) and (U vs I) Stokes polarization parameters (see Fig.6) and found that the entire data set can be split into two sections with its own behavior in (I, Q, U) parameter space. We mark these sections with the same colors as in Fig.2. Red regression lines in Fig.6 represent a component with constant parameters of polarization,  $P_{\text{comp}}$  and  $\theta_{\text{comp}}$ , while its total and polarized fluxes vary. The parameters of variable source acting during maximum of the flare are:  $p=47 \pm 0.7\%$ ,  $\theta=16.9^\circ \pm 1^\circ$ .

Fig.7 displays the observed dependencies between polarization parameters and flux density in R-band. The fractional polarization changes from 2% to 33%, while the flux varies from  $\sim 3$  mJy to 16 mJy. Bottom left panel of Fig.7 displays dependence between the degree of polarization and flux. The Spearman rank correlation coefficient is  $\rho=0.833$ , meaning that the values are related, with the degree of polarization rising along with the flux that agrees with a shock in jet model. However, the relation between polarization degree and flux is nonlinear and bends at the maximum flux level. This might occur due to changes in the viewing angle.

Bottom panel of Fig.2 shows a blowup of the most interesting time interval of the outburst (24-27 September). During these days intranight variability of EVPA is obvious. EVPA rotates smoothly about  $15^\circ$  every night in one direction. Intranight EVPA variations could indicate the presence of complex helical structure (see e.g. Larionov et al. (2010); Villata et al. (2007, 2009)): the finest structure is responsible for variations on smaller scales (hours), while the large-scale one affects weeks- and month-lasting activity.

## References

- Abdo, A. A., Ackermann, M., Ajello, M., et al. 2010, ApJS, 188, 405  
 Edelson, R. A., & Krolik, J. H. 1988, ApJ, 333, 646  
 Hagen-Thorn, V. A., & Marchenko, S. G. 1999, Baltic Astronomy, 8, 575  
 Larionov, V. M., Jorstad, S. G., Marscher, A. P., et al. 2008, A&A, 492, 389  
 Larionov, V. M., Villata, M., & Raiteri, C. M. 2010, A&A, 510, AA93  
 Raiteri, C. M., Villata, M., Larionov, V. M., et al. 2008, A&A, 491, 755  
 Hagen-Thorn, V. A., Efimova, N. V., Larionov, V. M., et al. 2009, Astronomy Reports, 53, 510  
 Hagen-Thorn, V. A., Larionov, V. M., Blinov, D. A., et al. 2013, Astronomy Reports, 57, 726  
 Jorstad, S. G., Marscher, A. P., Smith, P. S., et al. 2013, ApJ, 773, 147  
 Villata, M., Raiteri, C. M., Gurwell, M. A., et al. 2009, A&A, 504, L9  
 Villata, M., Raiteri, C. M., Aller, M. F., et al. 2007, A&A, 464, L5



<http://lacerta.astro.spbu.ru/?q=program>